http://journal.uir.ac.id/index.php/JGEET

E-ISSN : 2541-5794
P-ISSN : 2503-216X

Journal of Geoscience,
Engineering, Environment, and Technology
Vol 10 No 4 2025

RESEARCH ARTICLE

Tsunami Evacuation Route Optimization Based on Megathrust Scenario Modeling in Pangandaran, West Java, Indonesia

Mirda Prisma Wijayanto[1,*], Arifin Achmad[1], Muflihatun[1], Chiquita Laila Mahfud[1], Syafrida Dwi Apriyanti[1], Zulfa Siti Zakia[1]

[1] *Department of Physics, Faculty of Mathematics and Natural Sciences, Universitas Jenderal Soedirman, Jl. Dr. Seoparno no.61, Purwokerto, 53122, Indonesia.*

* Corresponding author : mirda.wijayanto@unsoed.ac.id
Tel.:+62-89-541-044-2539;
Received: July 4, 2025; Accepted: Dec 19, 2025.
DOI: 10.25299/jgeet.2025.10.4.23739

Abstract

The southern coastal area of West Java, particularly Pangandaran, faces a high risk of tsunami disasters triggered by megathrust earthquakes. However, current evacuation strategies in the region often lack integration between seismic hazard analysis, tsunami wave propagation modeling, and evacuation route optimization. To address this gap, this study aims to develop an integrated framework that combines seismicity assessment, tsunami simulation, and optimal evacuation planning for the Pangandaran coastal region. Seismic records from 2000 to 2024 indicate a total of 3090 earthquake events, predominantly offshore, with magnitudes ranging from low to moderate. The estimated b-value (1.19 ± 0.04) and a-value (8.057) reflect significant tectonic stress within the subduction zone between the Indo-Australian and Eurasian plates. Spatial analysis highlights offshore zones as areas of elevated seismic risk with the potential for large-magnitude events. Tsunami modeling was performed using the COMCOT model under a scenario of an 8.7 Mw megathrust earthquake. The simulation revealed maximum wave heights of up to 18.59 meters, reaching the coast within 40–45 minutes. Natural features such as coastal conservation zones were observed to reduce wave intensity, underscoring their role in hazard mitigation. Evacuation route modeling was carried out using Dijkstra's algorithm, with two designated starting points located in the eastern and western sectors of Pangandaran Beach. The optimal routes identified to a designated Temporary Evacuation Site (TES) produced travel distances of 1.093 km and 0.533 km, requiring 26.23 and 12.79 minutes respectively, both within the available time window before tsunami impact. The findings offer actionable input for local disaster preparedness and evacuation planning. Furthermore, this study demonstrates the practical application of graph theory in disaster mitigation and provides a scalable framework for tsunami-prone regions worldwide.

Keywords: Megathrust, Tsunami, Optimal Evacuation Routes, Pangandaran

1. Introduction

Megathrust earthquakes occur along subduction zones, where one tectonic plate is forced beneath another. Due to their potential to generate both seismic and tsunami hazards, making it crucial to understand their recurrence potential and associated risks. The southern Java megathrust has been identified as one such high-risk zone. Previous work by (Supendi et al., 2023) analyzed seismic data cataloged by the Indonesian Meteorology, Climatology, and Geophysics Agency (BMKG) and the International Seismological Center (ISC) for the period April 2009 to July 2020. By applying the double-difference teleseismic relocation method, they identified a substantial seismic gap extending across southern Java and southeastern Sumatra. This gap correlates with previous GPS studies, confirming that the region is a likely source of future megathrust earthquakes with tsunami-generating potential.

One of the areas most vulnerable to a future megathrust event in southern Java is the southern region of West Java (Pristiwantoro et al., 2025). This vulnerability arises from its tectonic setting, straddling the boundary between the oblique subduction of the Australian plate beneath Sumatra (Irwandi et al., 2025) and the orthogonal subduction beneath Java (DeMets et al., 2010). The seismic history of West Java underscores this risk. Newcomb and McCann (Newcomb and McCann, 1987) documented two major earthquakes in the region with magnitudes exceeding 7.5 in the years 1903 and 1921. More recently, a Mw 7.8 megathrust earthquake in 2006 (Ammon et al., 2006; Fujii and Satake, 2006; Gunawan et al., 2016; Hanifa et al., 2014) and a Mw 6.8 intraslab event in 2009 (Gunawan et al., 2019; Suardi et al., 2014) further demonstrate the area's seismic activity. According to (Jones et al., 2014), earthquakes caused by the southern Java megathrust generally have the potential to generate high tsunamis because they occur at shallow depths (less than 30 km). Based on historical records, one of the areas in West Java that could potentially experience a tsunami due to the megathrust is Pangandaran beach. To reduce the risk of disasters caused by the southern Java megathrust in the future, especially on the Pangandaran coastal area, tsunami disaster mitigation efforts are needed by determining the optimal tsunami evacuation route.

The planning of evacuation routes must account for both the seismic and tsunami hazards specific to the region. The level of seismic threat can be quantified using seismicity parameters such as the a-value and b-value derived from frequency–magnitude distributions. Several studies have analyzed the seismicity of Java island region based on these metrics (Arubi et al., 2022; Suananda Y. et al., 2018), providing insight into the stress accumulation

and earthquake recurrence potential in the area. In parallel, tsunami modeling is critical to understanding the spatial extent of tsunami impact. Modeling efforts related to the 2006 Pangandaran tsunami have been analyzed in previous studies (Priadi et al., 2020; Sriyanto et al., 2025), offering valuable input for defining hazard zones. However, integrating these analyses into evacuation route planning remains limited in current research.

Furthermore, one of the major challenges in disaster evacuation planning lies in the complexity of the transportation network, particularly the presence of numerous branching roads, intersections, and constrained pathways. These factors can lead to significant delays, traffic congestion, and confusion among evacuees, especially during high-stress emergency situations. As a result, determining optimal evacuation routes, which minimize travel time, avoid hazard zones, and account for infrastructure constraints, is essential for effective and timely disaster response.

Various methods have been developed to address this issue, broadly classified into graph-theoretical algorithms (Mayasari and Afandi, 2021; Péroche et al., 2014), heuristic approaches (Fathianpour et al., 2024; Ferreira et al., 2025; Laksono et al., 2022), and geospatial-based systems (Darmi et al., 2019; Tahri et al., 2025). In the realm of graph theory, the Dijkstra algorithm is one of the most widely used due to its ability to determine the shortest path in a weighted graph with non-negative edges. Beyond these algorithmic techniques, Geographic Information Systems (GIS) have become a powerful tool in evacuation route planning. Platforms such as ArcGIS Network Analyst, QGIS, and GRASS GIS allow for the incorporation of spatial data, elevation models, land use, population density, and hazard zones into route optimization models. Altogether, the selection of an appropriate method depends on multiple factors, including data availability, computation time, network complexity, and the specific disaster scenario. For this reason, Dijkstra's algorithm offers a robust, computationally efficient, and practically implementable solution for evacuation route optimization in tsunami-prone regions such as Pangandaran.

Despite numerous studies addressing hazard mitigation in Pangandaran, none to date have integrated megathrust earthquake scenario, tsunami modeling, and evacuation route optimization into a single comprehensive framework. This research addresses this gap by developing an integrated model that combines (1) megathrust earthquake modeling, (2) tsunami modeling using the Cornell Multi-grid Coupled Tsunami (COMCOT), and (3) evacuation route optimization employing a Dijkstra algorithm. The novelty of this study lies in the integration of these three components. This integrated framework not only improves the accuracy and effectiveness of evacuation planning in tsunami-prone areas but also contributes scientifically by demonstrating a scalable methodology that can be applied to other coastal regions vulnerable to megathrust hazards.

2. Methodology

This section outlines the methodological framework, data sources, and computational tools employed in the research. An overview of the research flowchart is illustrated in the flowchart presented in Figure 1.

The study began with earthquake modeling to assess the seismic activity analysis of the study area. This was performed by calculating two key seismic parameters: the b- and a-values. The b-value represents the slope of the logarithmic linear relation between the frequency of events and their magnitudes, defined as follows:

$$b = \frac{1}{\bar{M} - M_{min}} \log e \tag{1}$$

where $\bar{M}$ is the average magnitude of the events, and M_{min} is the minimum magnitude used in the analysis. In addition, the a-value represents the overall level of seismic activity, which can be defined as follows:

$$a = 10 \log(N) + b.M_{min} \tag{2}$$

where N is the total number of events with magnitude $\geq M_{min}$. Following the previous works (Kijko, 1988; Kijko and Sellevoll, 1990), these values were computed using the Maximum Likelihood Estimation (MLE) method implemented in the ZMAP toolbox for MATLAB. The input data consisted of daily earthquake magnitude records for the southern region of West Java, bounded by the coordinates latitude of [10°35'45.60", 7°3'25.20"] and longitude of [106°19'33.60", 108°47'13.20"], covering the period from 2000 to 2024. The earthquake data were obtained from the United States Geological Survey (USGS) as secondary sources.

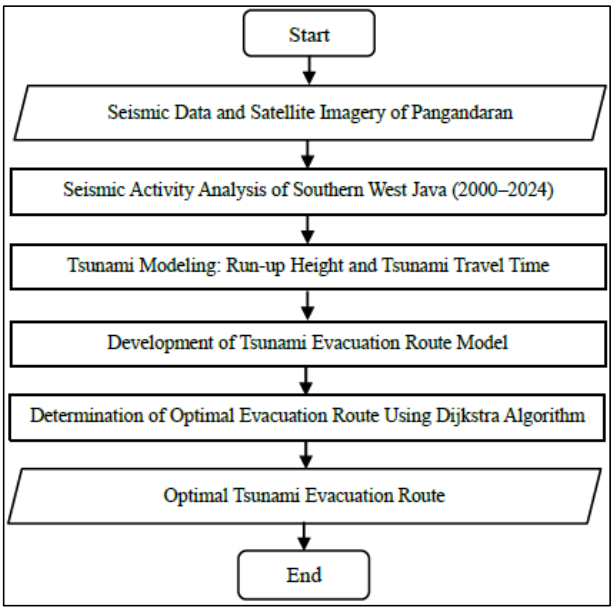

Fig 1. Flowchart of the research methodology

The calculated b- and a-values provide an estimate of the regional seismicity level and serve as indicators of the likelihood and frequency of future megathrust events. Moreover, seismic activity patterns derived from these values offer a preliminary insight into the tsunami-generating potential of earthquakes in the study region.

Next, the earthquake source parameters were derived from the megathrust source zone. These additional parameters were estimated based on empirical relationships between moment magnitude (M_w), fault length (L), and fault width (W), using the formulations developed by Wells & Coppersmith (1994) and Hanks & Kanamori (1979). These equations were employed to calculate the seismic moment (M_o) and average slip displacement (D) as follows:

$$\log L = 0.58\, M_W - 2.42, \tag{3}$$
$$\log W = 0{,}41\, M_W - 1.61, \tag{4}$$
$$M_W = \frac{2}{3}\log(M_0) - 10.7, \tag{5}$$

$$M_0 = \mu DA, \quad (6)$$

where μ is the shear modulus of the fault zone rock (typically 3×10^{11} dyne/cm^2) and A denotes the fault rupture area (m^2). These formulations provide a means to derive earthquake parameters based on physical fault characteristics and seismic energy release.

The derived parameters were subsequently used as input for tsunami modeling simulations performed using the Cornell Multi-grid Coupled Tsunami (COMCOT) software. Moreover, the tsunami model yielded three critical parameters:

a. Tsunami run-up, representing the maximum vertical height of the tsunami wave as it reaches the shore;
b. Tsunami travel time, defining the time interval between the earthquake event and the arrival of the tsunami at the nearest coastal point.

The outputs of the tsunami simulation were then used as foundational inputs for the evacuation route modeling. In order for the research to be focused on answering the research questions, we give the following research limitations:

a. Tsunami evacuation route modeling was only carried out in the Pangandaran coastal area.
b. The starting point of evacuation is only focused on Pangandaran beach which consists of two locations, namely the eastern and western sectors of Pangandaran beach.
c. The evacuation routes to be chosen are several highways with the following conditions:
   1) The route has space to run 1 m^2/person.
   2) The route is far enough from the coastline and lead to a safe point or evacuation destination point.
   3) The evacuation route determination analysis does not take into account the number of residents.
d. The selected road intersections are those that connect several highways selected as evacuation routes.
e. Evacuation safe points location must have a height of more than the predicted maximum height of a tsunami generated by the megathrust.

Evacuation route modeling begins with determining evacuation safe points. An evacuation safe point is a temporary evacuation site (TES) that is intended to be able to evacuate the entire tsunami-exposed population in an area to survive the tsunami. A temporary evacuation site (TES) has been built by the Pangandaran Regency government. The TES is located in Pasar Wisata block, Pangandaran village with a latitude of 7°41'30.37" and a longitude of 108°39'13.85".

The selection of Dijkstra's algorithm in this study is based on its computational efficiency, accuracy, and widespread application in network-based path optimization problems. Dijkstra's algorithm is particularly suitable for tsunami evacuation modeling due to its ability to compute the shortest path on weighted graphs with non-negative edge values, which aligns with the nature of urban road networks. Compared to heuristic approaches such as A*, genetic algorithms, or fuzzy Dijkstra variants, Dijkstra's method ensures deterministic results and guarantees the global optimum, making it appropriate for critical disaster response planning where uncertainty should be minimized. Furthermore, the algorithm is straightforward to implement, requires relatively low computational resources, and can be easily integrated with GIS-based spatial data. These characteristics make Dijkstra's algorithm a robust and practical choice for identifying optimal evacuation routes in real-time scenarios under urgent conditions such as tsunami threats.

The next steps in processing and analyzing the research data are as follows:

a. Creating an evacuation route graph model consisting of a collection of vertices $\{A, B, C, D, E, F, \dots\}$ and a collection of edges with graph weights $\{1,2,3,4,5,8, \dots\}$.
b. Determining the latitude and longitude coordinates for each vertice of the graph.
c. Calculating the coordinate length (ΔL) with the formula:

$$\Delta L = \sqrt{(LA_2 - LA_1)^2 + (LO_2 - LO_1)^2} \quad (7)$$

where:
LA_2 = Latitude measurement value of node 1
LA_1 = Latitude measurement value of node 2
LO_2 = Longitude measurement value of node 1
LO_1 = Longitude measurement value of node 2

d. Converting the coordinate difference unit to km (kilometer) by using the formula:

$$\Delta L' = \Delta L \times 111.32\ km \quad (8)$$

e. Calculating the distance between graph vertices (JS) by using the formula:

$$JS = \Delta L' - \Delta L \quad (9)$$

f. Tabulating the research data
Determining the optimal evacuation route based on Dijkstra's algorithm using MATLAB.

3. Result and Discussion

The structure of this section reflects the methodological framework established in Section 2, wherein the study is divided into three main components: seismicity analysis, tsunami wave propagation modeling, and evacuation route optimization. Each subsection corresponds directly to the respective stage in the methodology, allowing for a clear traceability between the methods employed and the outcomes obtained. This alignment ensures that the analytical procedures are not only transparently reported but also scientifically justified in terms of how each modeling technique contributes to the overall objective of improving tsunami disaster mitigation in Pangandaran.

3.1 Earthquake modeling

Tsunamis are among the most devastating natural hazards, often triggered by undersea earthquakes (Faiez and Fan, 2023; Khusnani et al., 2024). As such, understanding the seismic characteristics of a region is a crucial prerequisite for tsunami modeling (Iqbal et al., 2023). Key seismic parameters relevant to tsunami generation include earthquake frequency, seismicity indices (b-value and a-value), and the earthquake source parameters.

This study begins with an examination of earthquake occurrence in the southern region of West Java. Between 2000 and 2024, a total of 3090 seismic events were recorded in the area, based on data from the United States Geological Survey (USGS). As shown in Figure 2, spatial analysis using QGIS v3.28.2 indicates that most earthquakes were located offshore, with magnitudes ranging from 3.3 to 7.7 Mw.

Further insights into the frequency–magnitude distribution (Figure 3) reveal that magnitude 4.5 Mw events were the most prevalent, comprising 210 occurrences. While most events were of low to moderate magnitude, the high event density underscores ongoing tectonic stress and indicates a potential risk of larger-magnitude earthquakes in the future.

Furthermore, the b-value and a-value, which serve as key seismicity indicators, were estimated using the maximum likelihood approach to ensure statistical robustness in characterizing earthquake frequency–magnitude relationships. Prior to this, a declustering process using the Reasenberg algorithm (Karapetyan et al., 2024; Reasenberg, 1985) was performed to remove dependent events such as foreshocks and aftershocks, isolating mainshocks for statistical reliability. The resulting b-value of 1.19 ± 0.04 suggests a typical seismic environment, where small-magnitude events dominate over larger ones. A b-value near 1.0 is commonly associated with regions of elevated tectonic stress. The computed a-value of 8.057 indicates a high overall level of seismic activity, consistent with the region's proximity to the Indo-Australian–Eurasian plate boundary.

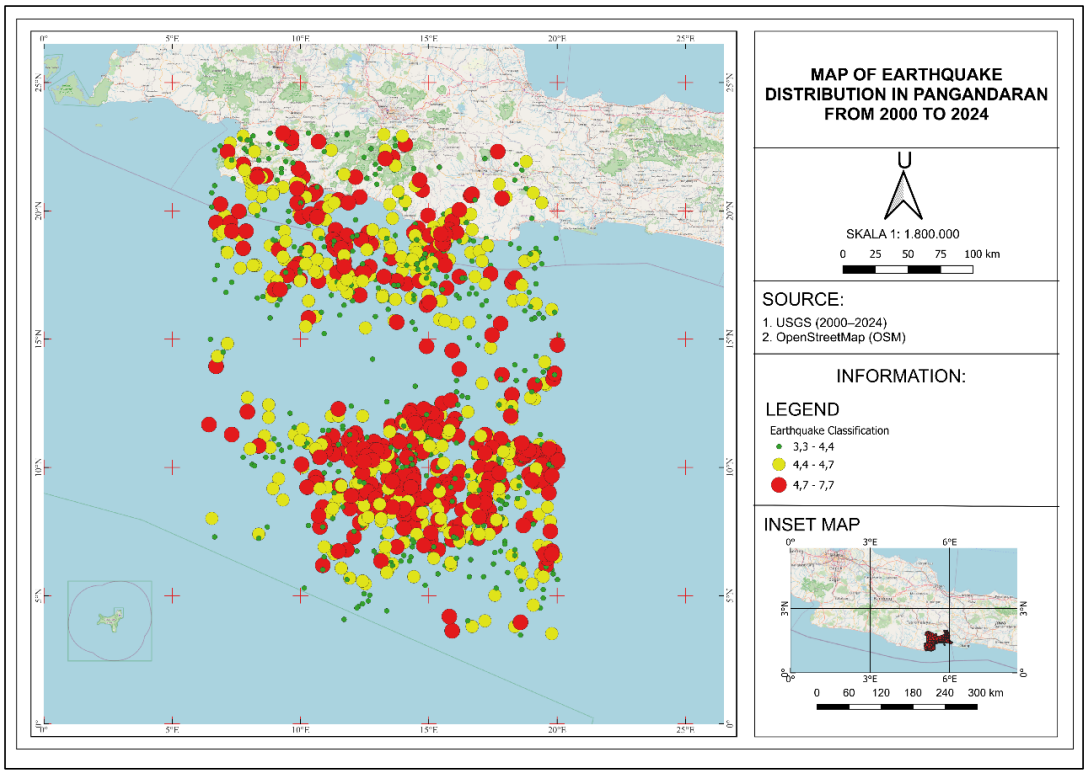

Fig 2. Spatial distribution of earthquakes in southern region of West Java.

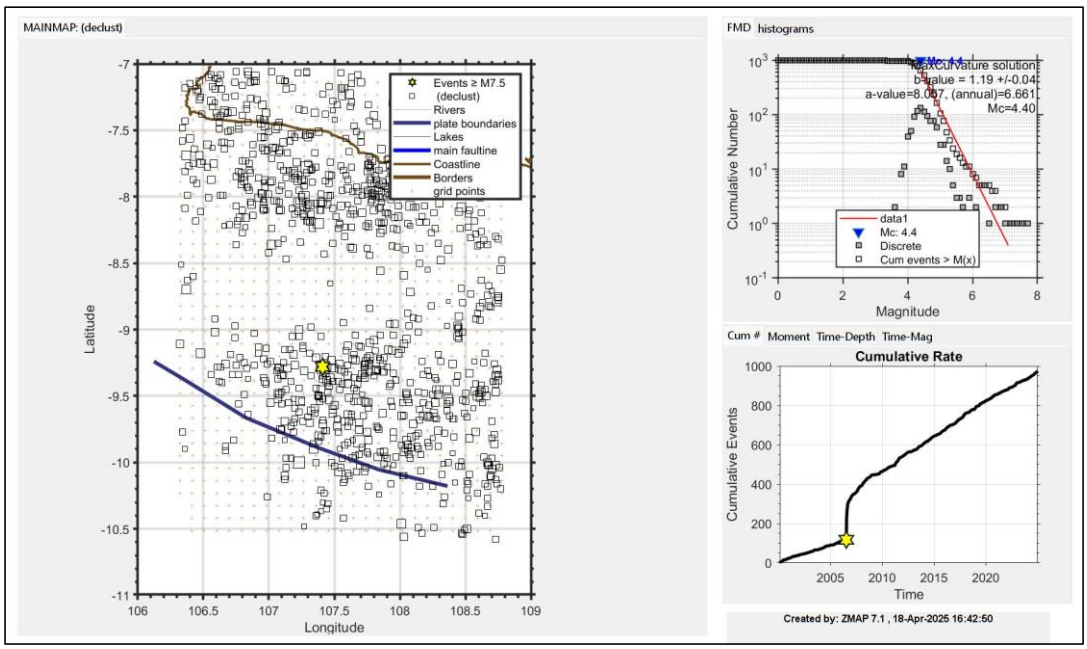

Fig 3. Frequency–magnitude distribution and cumulative event rate of earthquakes between 2000–2024.

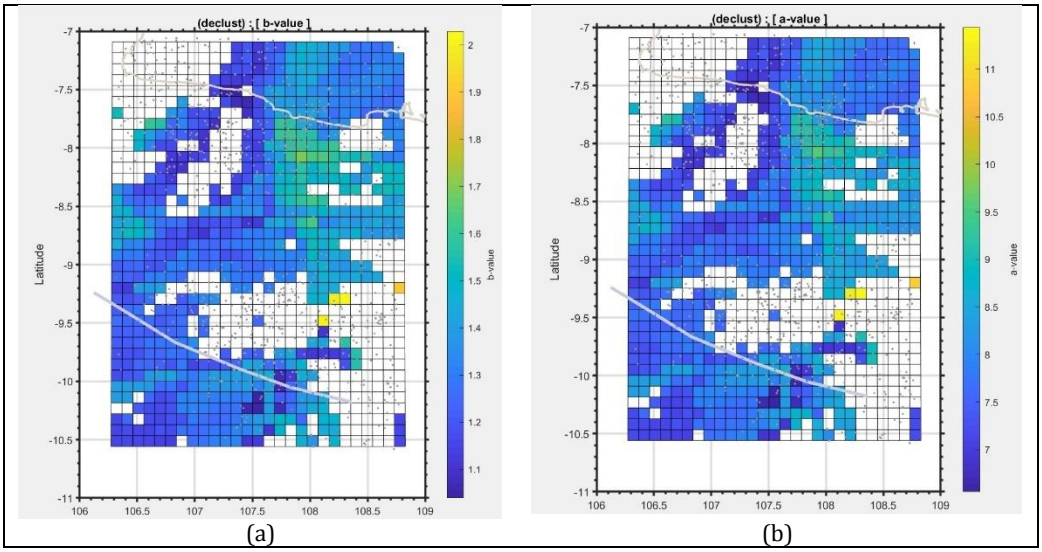

Fig 4. Spatial variation of (a) b-value and (b) a-value across southern region of West Java.

Spatial variations of both parameters are illustrated in Figure 4. The b-value map ranges from 1.1 (dark blue) to 2.0 (bright yellow), where lower values denote zones of higher stress accumulation and potential for large earthquakes. Conversely, higher b-values represent areas where stress is released more frequently via small events. The a-value map shows values ranging from 7.0 (dark blue) to 11.0 (bright yellow), with the highest concentrations offshore, further confirming the influence of the subduction zone on regional seismicity.

The subsequent section focuses on the characterization of earthquake source parameters associated with the megathrust zone located off the southern region of West Java. The scenario is based on a representative seismic event with a moment magnitude of 8.7 Mw, as reported by Pusgen and supported by the USGS Slab 2.0 model. The earthquake hypothetical epicenter is positioned at a latitude of 9°19'8.40" and a longitude of 108°35'38.40" at a depth of 21 km. A fault slip angle of 90° was applied to represent a worst-case scenario for tsunami inundation. The rupture mechanism is further defined by a strike of 290.38° and a dip of 11.17°, consistent with subduction zone geometry. Using these parameters, the earthquake source characteristics were then calculated based on empirical relationships described in Eqs. (3)–(6), yielding the values presented in the following table.

Table 1. Earthquake source parameters associated with the megathrust zone located off the southern region of West Java.

MW	$L\ (km)$	$W\ (km)$	$D\ (m)$	$M_0\ (Nm)$
8,7	423	91	20	5.62×10^{23}

The earthquake source parameters summarized in Table 1 serve as the basis for tsunami simulation and will be utilized as input data in the numerical modeling described in the subsequent subsection.

3.2 Tsunami Modeling

The COMCOT (Cornell Multi-grid Coupled Tsunami) model was selected for this study due to its proven capability in simulating both deep-ocean wave propagation and nearshore inundation with high accuracy. COMCOT integrates linear and nonlinear shallow water equations, enabling it to simulate tsunami generation, propagation, and run-up effectively across varying bathymetric and coastal topographies (Felix et al., 2024; Harig et al., 2022; Sihombing et al., 2024; Windupranata et al., 2020). Compared to other numerical models such as TUNAMI-N2 or MOST, COMCOT offers a flexible multilayer grid system and has been successfully validated in several Indonesian tsunami events, including the 2004 Aceh and 2006 Pangandaran tsunamis (Tri Laksono et al., 2020). Its implementation is also supported by global datasets for bathymetry and has been widely adopted in academic and governmental hazard assessments. These strengths make COMCOT a robust and context-appropriate choice for tsunami hazard modeling in Indonesia's tectonically active coastal regions.

In the tsunami modeling, we use a two-layer grid with the following configuration. Layer 1 represents the open ocean domain to capture the propagation of tsunami waves at a broad scale, while Layer 2 provides a finer resolution domain nested within Layer 1. Both of these layers utilize bathymetric and topographic data sourced from the ETOPO global dataset. The geographic boundaries, grid resolutions, and distance point for each layer used in the tsunami model are summarized in Table 2.

Table 2. Layers configuration of the tsunami modeling.

Layer	Latitude	Longitude	Resolution (arc sec)	Distance Point (m)
1	7°11'17.54" - 9°50'56.06"	106°3'47.52" - 110°57'12.24"	17.69	540
2	7°24'1.52" - 8°30'38.96"	107°40'12.62" - 109°33'40.94"	5.89	180

Tsunami modeling was carried out using the COMCOT (Cornell Multi-grid Coupled Tsunami) model, with input parameters derived from Table 1 and Table 2. The simulation, based on an earthquake scenario of magnitude 8.7 Mw, was performed over a duration of 120 minutes (2 hours) with a time step interval of 1 seconds. Snapshots of tsunami wave propagation were generated at various grid levels. Figure 4 presents the tsunami simulation of the model. Shortly after the earthquake event, a noticeable sea level depression occurred, visualized as a blue shift on the color scale. At minute 34, tsunami waves approached the shoreline, and by minute 120, inundation had reached all of the Pangandaran coastal area.

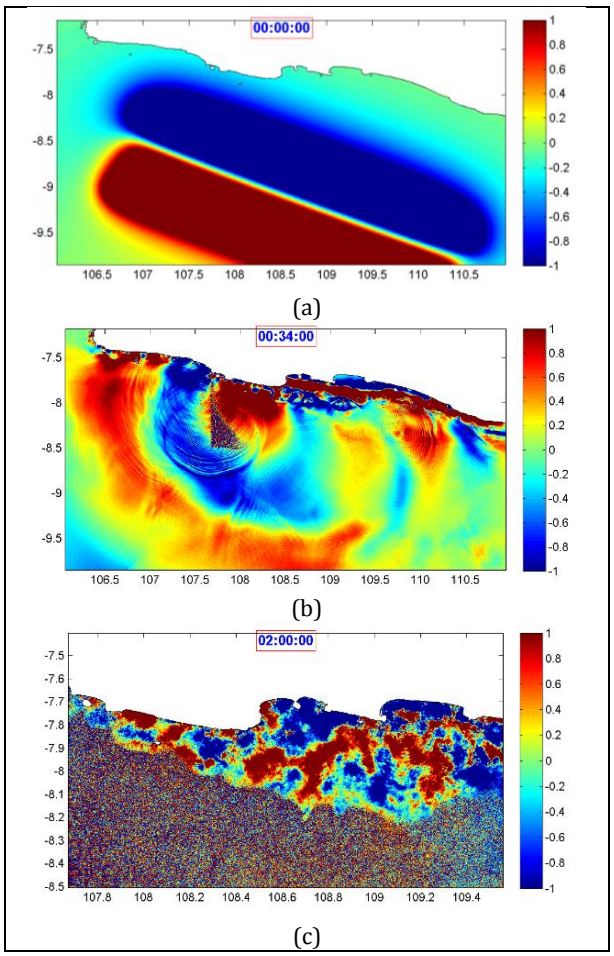

Fig 5. Tsunami wave propagation at different simulation times: (a) initial condition (0 minutes); (b) wave approaching the shoreline (34 minutes); and (c) coastal inundation phase (120 minutes).

In the tsunami modeling, three virtual tide gauges (TGVs) were strategically deployed to monitor wave height and tsunami arrival time. TGV-1 was positioned at coordinates 7°41'28.39" and 108°43'49.12"; TGV-2 at 7°44'10.67" and 108°40'7.65"; and TGV-3 at 7°41'12.19" and 108°35'52.68". The tsunami travel time histories recorded at each tide gauge location are illustrated in the following figures.

As illustrated in Figure 6, the maximum tsunami wave height recorded by TGV-1 was 18.58881 meters, with the peak occurring at 45 minutes and 23 seconds after the initial earthquake. At TGV-2, the maximum recorded height was 8.77095 meters, reached at 40 minutes and 26 seconds, while TGV-3 recorded a maximum height of 16.0991 meters at 42 minutes and 13 seconds. The variation in arrival time and wave height is primarily influenced by bathymetric depth and the coastal slope of each location.

Among the three stations, TGV-2 registered the lowest tsunami height. This is likely attributed to the presence of a nature reserve in the vicinity, which acts as a natural breakwater, thereby attenuating the tsunami energy before it reaches the shore. These findings align with previous studies (Benazir et al., 2024), which have shown that natural coastal features such as conservation areas, mangrove forests, and other vegetated barriers can effectively reduce tsunami impact by lowering wave heights and dissipating energy. Given the significant tsunami wave heights observed at TGV-1 and TGV-3, located on the eastern and western sectors of Pangandaran beach, respectively, both of which are densely populated areas, tsunami evacuation route modeling will be prioritized for these two regions. The evacuation modeling approach and results will be presented in the following subsection.

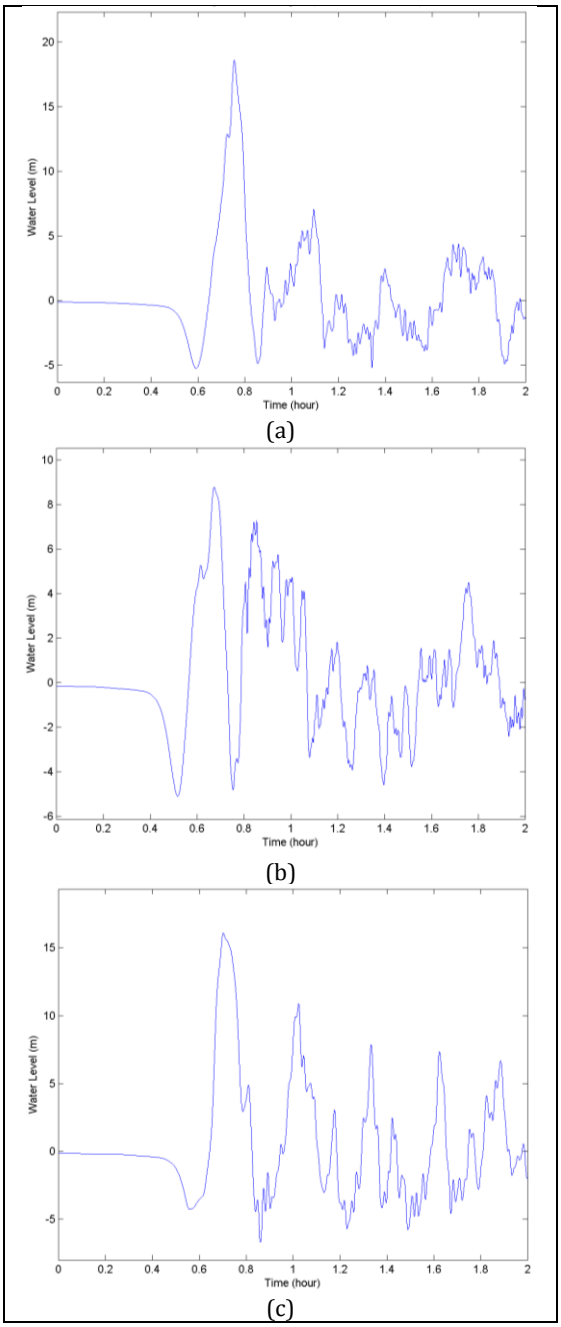

Fig 6. The tsunami travel time histories were recorded by: (a) TGV-1; (b) TGV-2; and (c) TGV-3.

3.3 Evacuation Routes Modeling

Pangandaran beach is divided into two sectors, namely the eastern and western sectors. The selected starting point location of the eastern sector is located at a latitude of 7°41'46.44" and a longitude of 108°39'37.30". While the starting point location chosen on the western sector is located at a latitude of 7°41'46.06" and a longitude of 108°39'14.74". Both locations are densely populated locations and locations most frequently visited by tourists.

The determination of tsunami evacuation points is carried out by determining the point with the lowest level of vulnerability of tsunami disaster mitigation evacuation sites include elevation, land use, slope, distance from the

coast, and distance from the river. In addition, the determination of the location of tsunami evacuation endpoints must also consider tsunami parameters as described in the previous subsections. Thus, the location of tsunami evacuation endpoint must fulfill the following criteria:

a. The evacuation site building must withstand the shaking of an 8,7 MW earthquake.
b. The location of the evacuation endpoint must be more than 18 meters in height as the maximum tsunami height based on the model.
c. The evacuation time from the starting point to the evacuation end point should be less than 40 minutes, which is the time to reaching the tsunami maximum height.

By considering the above criteria, we propose that the tsunami evacuation shelter be located at the TES (Temporary Evacuation Site) Building located at Pasar Wisata block, Pangandaran village with a latitude of 7°41'30.37" and a longitude of 108°39'13.85". The building was built by the Pangandaran Regency Government and the Ministry of PUPR. The building has three floors, with a size of 50 $m \times 60$ m and is able to accommodate up to around 6.000 people, enough to accommodate more than half of the total population of Pangandaran village who are potentially affected.

Before determining the evacuation route, we firstly select the locations that will become vertice points of the graph model. The location of the selected vertices can be seen in the table 3.

Table 3. List of the vertice points

Vertices	Latitude	Longitude
V1	7°41'46.44"	108°39'37.30"
V2	7°41'45.73"	108°39'37.75"
V3	7°41'34.79"	108°39'45.84"
V4	7°41'46.94"	108°39'33.22"
V5	7°41'45.85"	108°39'33.66"
V6	7°41'44.43"	108°39'34.19"
V7	7°41'38.71"	108°39'34.96"
V8	7°41'36.53"	108°39'34.62"
V9	7°41'32.60"	108°39'33.75"
V10	7°41'46.81"	108°39'28.16"
V11	7°41'43.93"	108°39'28.32"
V12	7°41'41.00"	108°39'28.36"
V13	7°41'38.01"	108°39'28.54"
V14	7°41'36.76"	108°39'28.48"
V15	7°41'33.20"	108°39'28.66"
V16	7°41'45.63"	108°39'22.17"
V17	7°41'41.68"	108°39'22.27"
V18	7°41'39.56"	108°39'22.24"
V19	7°41'35.04"	108°39'22.59"
V20	7°41'33.61"	108°39'22.79"
V21	7°41'44.73"	108°39'17.67"
V22	7°41'41.41"	108°39'17.99"
V23	7°41'33.79"	108°39'21.25"
V24	7°41'34.15"	108°39'17.75"
V25	7°41'46.06"	108°39'14.74"
V26	7°41'44.29"	108°39'13.10"
V27	7°41'42.31"	108°39'14.97"
V28	7°41'34.53"	108°39'14.98"
V29	7°41'29.71"	108°39'20.70"
V30	7°41'29.93"	108°39'16.14"
V31	7°41'30.37"	108°39'13.85"

Descriptions:

V1: Starting point from the eastern sector of Pangandaran beach
V2: T-junction of Street Pantai Timur – RM Risma Seafood
V3: T-junction of Street Pantai Timur – Pengadilan lama
V4: The corner of pondok Zio
V5: T-junction of pondok Abah Sudir
V6: Street intersection of Gg. Tongkol – Becak Pasar Ikan
V7: T-junction of Street Ps. Ikan – Pondok Cepot New
V8: T-junction of Street Ps Ikan – Street Tembusan
V9: Street intersection of Street Ps. Ikan – Pengadilan Lama
V10: T-junction of Kidang Pananjung – Street Pramuka
V11: T-junction of Street Kidang Pananjung – Gg. Tongkol
V12: T-junction of Street Kidang Pananjung – Gg. Kakap
V13: T-junction of Kidang Pananjung – Street Tembusan
V14: Intersection of Street Kidang Pananjung – Pondok SBC
V15: Intersection of Street Kidang Pananjung – Bulak Laut
V16: Street intersection of Street Pramuka – Kalen Buaya
V17: T-junction of Street Jangilus – CV. Dua Putra Jaya Sejahtera
V18: T-junction of Street Jangilus – Gg. Kakap
V19: T-junction of Street Jangilus – Althatrans Travel
V20: T-junction of Street Jangilus – Street Bulak Laut
V21: T-junction of Street Sumardi – Street Pramuka
V22: T-junction of Street Sumardi – Sinar Rahayu 4
V23: T-junction of Street Bulak Laut – Tourist Market
V24: T-junction of Street Bulak Laut – Street Sumardi
V25: Starting point from the western sector of Pangandaran Beach
V26: T-junction of Street Pamugaran Bulak Laut – Susi Travel
V27: T-junction of Pondok Penginapan Moruya
V28: T-junction of Pangandaran Beach Information Center
V29: The northeast corner of the Tourist Market
V30: Tourist market bend to evacuation endpoint
V31: Evacuation endpoint

The vertices will then be interconnected to form an evacuation route graph model as shown in figure 7.

Fig 7. Graph model of Pangandaran tsunami evacuation routes.

Based on the Figure 7, we can calculate the graph weight that represents distance between the vertices as follows:

Table 4. Distance between the vertices

No.	Starting Point	Endpoint	Distance (m)
1	V1	V2	25.99
2	V1	V5	114.02
3	V2	V3	420.74
4	V2	V6	117.19
5	V3	V9	1612.18
6	V4	V5	36.34
7	V4	V10	156.52
8	V5	V6	36.37
9	V6	V7	178.47
10	V6	V11	182.17
11	V7	V8	68.22
12	V7	V13	199.70
13	V8	V9	124.46
14	V8	V14	198.99
15	V9	V15	158.48
16	V10	V11	89.19

17	V10	V16	188.70
18	V11	V12	90.62
19	V11	V17	199.60
20	V12	V13	92.62
21	V12	V18	194.41
22	V13	V14	38.69
23	V14	V15	110.22
24	V14	V19	189.74
25	V15	V20	181.95
26	V16	V17	122.18
27	V16	V21	141.90
28	V17	V18	65.56
29	V17	V22	132.61
30	V18	V19	140.18
31	V19	V20	44.64
32	V20	V23	47.94
33	V21	V22	103.13
34	V21	V25	99.50
35	V22	V24	224.62
36	V22	V27	97.44
37	V23	V24	108.80
38	V23	V29	231.32
39	V24	V28	86.45
40	V24	V30	139.66
41	V25	V26	74.61
42	V26	V27	84.21
43	V27	V28	240.57
44	V28	V31	133.29
45	V29	V30	141.17
46	V30	V31	72.10
47	V31	V28	133.29

In the next step. we employ Dijkstra's algorithm using MATLAB to determine the evacuation route with the shortest distance which is defined as the route with the minimum number of weights. Output of the program can be shown in Figure 8 below:

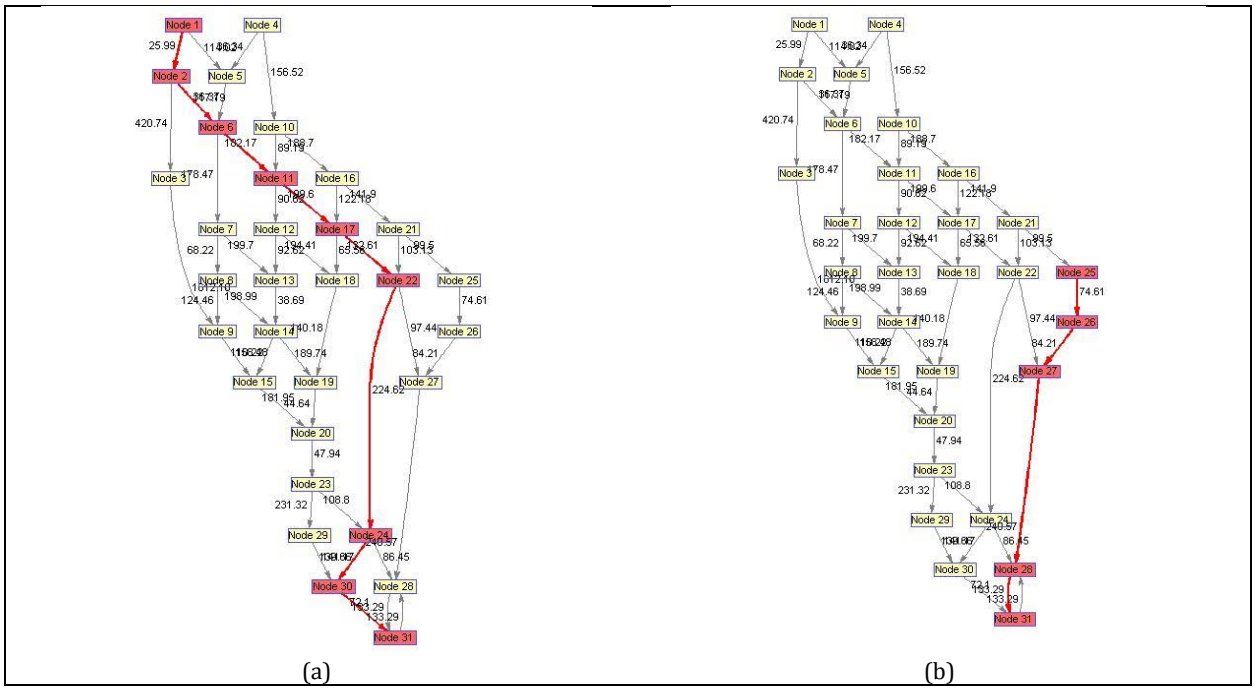

Fig 8. Evacuation route model at: (a) the eastern; and (b) the western sector of Pangandaran beach.

We assume that the average speed of people walking is 2.5 $km/hour$ and is constant. Then. based on Figure 8. the optimal evacuation route is obtained as follows:

1. Evacuation route model from the starting point of eastern sector of Pangandaran beach (V1) to the evacuation site (V31) can be summarized as follows:
   a. Evacuation route: V1 → V2 → V6 → V11 → V17 → V22 → V24 → V30 → V31
   b. Total evacuation distance: 1.093 km.
   c. Total evacuation time: 26.23 minutes.
2. Evacuation route model from the starting point of western sector of Pangandaran beach (V25) to the evacuation site (V31) can be summarized as follows:
   a. Evacuation route: V25 → V26 → V27 → V28 → V31
   b. Total evacuation distance: 0.533 km.
   c. Total evacuation time: 12.79 minutes.

The evacuation route modeling using Dijkstra's algorithm successfully identified the shortest and fastest paths from both the eastern and western sectors of Pangandaran beach to the designated evacuation site. The results show that the evacuation times, 26.23 minutes from the eastern sector (1.093 km) and 12.79 minutes from the western sector (0.533 km), are well within the estimated tsunami arrival time, indicating that the routes are feasible for timely evacuation. These findings provide valuable insights for local disaster management authorities in developing effective tsunami mitigation strategies, particularly for high-risk and densely populated coastal areas.

Several studies have explored alternative algorithms for evacuation route optimization (Ashar et al., 2018; Forcael et al., 2014; Mayasari and Afandi, 2021; Péroche et al., 2014; Sularno et al., 2021). Some widely used methods include the A* algorithm, fuzzy Dijkstra, and agent-based models. The A* algorithm is known for its speed and efficiency due to heuristic guidance, but it may not always guarantee the shortest global path in complex networks without carefully defined heuristics (Zikky, 2016). Fuzzy Dijkstra enhances flexibility by incorporating uncertainty and varying weights, such as crowd density or road conditions, but it requires subjective parameter tuning that may complicate implementation (Mayasari and Afandi, 2021). Agent-based models offer dynamic simulation of individual behaviors during evacuation; however, they demand extensive computational resources and detailed behavioral data (Kim et al., 2022), which are often unavailable in real-time

disaster scenarios. In contrast, Dijkstra's algorithm offers deterministic results, computational simplicity, and scalability, making it a reliable choice for static evacuation network modeling under tsunami threat. Given the urgency and infrastructure constraints in coastal areas like Pangandaran, the Dijkstra algorithm remains a robust and justifiable option for preliminary evacuation planning.

However, it is important to note that the current model does not account for several real-world constraints such as road width, surface quality, and population density, all of which may significantly influence actual evacuation efficiency. Incorporating these factors would be a valuable direction for future research to enhance the accuracy and applicability of evacuation planning models.

4. Conclusion

This study demonstrates an integrated framework that combines seismic hazard analysis, tsunami wave modeling, and evacuation route optimization for the tsunami-prone region of Pangandaran. The results confirm that the simulated megathrust scenario (Mw 8.7) poses a significant threat, with tsunami waves reaching the coast within 40–45 minutes. Through COMCOT simulation and Dijkstra-based routing, we identified evacuation paths with travel times of 12.79 and 26.23 minutes, well within the critical window for evacuation.

These findings validate the feasibility of the proposed approach for early-stage tsunami risk mitigation planning. The integration of seismic, tsunami, and routing models provides a scalable methodology applicable to other high-risk coastal zones. Future research may incorporate population dynamics, infrastructure constraints, and real-time simulation to further enhance evacuation planning accuracy and resilience.

Acknowledgements

This research was funded by the BLU Research Grant from Universitas Jenderal Soedirman under the RPK (Riset Peningkatan Kompetensi) scheme for the year 2025. Grant No. 14.505/UN23.34/PT.01/V/2025.

References

Ammon, C.J., Kanamori, H., Lay, T., Velasco, A.A., 2006. The 17 July 2006 Java tsunami earthquake. Geophys. Res. Lett. 33, 2006GL028005. https://doi.org/10.1029/2006GL028005

Arubi, D., Zulfakriza, Rosalia, S., Sahara, D.P., Puspito, N.T., 2022. Estimation of B-Value Variation as Earthquake Precursor in Java Region with Maximum Likelihood Method. IOP Conf. Ser. Earth Environ. Sci. 1047, 012027. https://doi.org/10.1088/1755-1315/1047/1/012027

Ashar, F., Amaratunga, D., Haigh, R., 2018. Tsunami Evacuation Routes Using Network Analysis: A case study in Padang. Procedia Eng. 212, 109–116. https://doi.org/10.1016/j.proeng.2018.01.015

Benazir, Triatmadja, R., Syamsidik, Nizam, Warniyati, 2024. Vegetation-based approached for tsunami risk reduction: Insights and challenges. Prog. Disaster Sci. 23, 100352. https://doi.org/10.1016/j.pdisas.2024.100352

Darmi, Y., Soerowirdjo, B., Wibowo, E., Ernastuti, 2019. Dijkstra algorithm application to determine the evacuation routes simulation earthquake and tsunami in the City Bengkulu based on GIS. J. Adv. Res. Dyn. Control Syst. 11, 1871–1887.

DeMets, C., Gordon, R.G., Argus, D.F., 2010. Geologically current plate motions. Geophys. J. Int. 181, 1–80. https://doi.org/10.1111/j.1365-246X.2009.04491.x

Faiez, Z., Fan, D., 2023. Study of Coastal Morphological Changes by Tsunamis in Aceh (Indonesia) Using Satellite Images. J. Geosci. Eng. Environ. Technol. 8, 295–304. https://doi.org/10.25299/jgeet.2023.8.4.12757

Fathianpour, A., Evans, B., Babaeian Jelodar, M., Wilkinson, S., 2024. Environmental factors in tsunami evacuation simulation: topography, traffic jam, human behaviour. Nat. Hazards 120, 12797–12815. https://doi.org/10.1007/s11069-024-06714-x

Felix, R., Hubbard, J., Wilson, K., Switzer, A., 2024. Heatmap analysis of modeled coastal tsunamis using different bathymetry data resolutions. Geosci. Lett. 11. https://doi.org/10.1186/s40562-024-00362-6

Ferreira, M.A., Oliveira, C.S., Francisco, R., 2025. Tsunami risk mitigation: the role of evacuation routes, preparedness and urban planning. Nat. Hazards 121, 6719–6751. https://doi.org/10.1007/s11069-024-07061-7

Forcael, E., González, V., Orozco, F., Vargas, S., Pantoja, A., Moscoso, P., 2014. Ant Colony Optimization Model for Tsunamis Evacuation Routes. Comput.-Aided Civ. Infrastruct. Eng. 29, 723–737. https://doi.org/10.1111/mice.12113

Fujii, Y., Satake, K., 2006. Source of the July 2006 West Java tsunami estimated from tide gauge records. Geophys. Res. Lett. 33, 2006GL028049. https://doi.org/10.1029/2006GL028049

Gunawan, E., Meilano, I., Abidin, H.Z., Hanifa, N.R., Susilo, 2016. Investigation of the best coseismic fault model of the 2006 Java tsunami earthquake based on mechanisms of postseismic deformation. J. Asian Earth Sci. 117, 64–72. https://doi.org/10.1016/j.jseaes.2015.12.003

Gunawan, E., Widiyantoro, S., Marliyani, G.I., Sunarti, E., Ida, R., Gusman, A.R., 2019. Fault source of the 2 September 2009 Mw 6.8 Tasikmalaya intraslab earthquake, Indonesia: Analysis from GPS data inversion, tsunami height simulation, and stress transfer. Phys. Earth Planet. Inter. 291, 54–61. https://doi.org/10.1016/j.pepi.2019.04.004

Hanifa, N.R., Sagiya, T., Kimata, F., Efendi, J., Abidin, H.Z., Meilano, I., 2014. Interplate coupling model off the southwestern coast of Java, Indonesia, based on continuous GPS data in 2008–2010. Earth Planet. Sci. Lett. 401, 159–171. https://doi.org/10.1016/j.epsl.2014.06.010

Harig, S., Zamora, N., Gubler, A., Rakowsky, N., 2022. Systematic Comparison of Tsunami Simulations on the Chilean Coast Based on Different Numerical Approaches. GeoHazards 3, 345–370. https://doi.org/10.3390/geohazards3020018

Iqbal, M., Denhi, A.D.A., Kristianto, Prayoga, A., 2023. Morphological Analysis of Anak Krakatau Volcano after 22 December 2018 Eruption using Differential Interferometry Synthetic Aperture Radar (DInSAR). J. Geosci. Eng. Environ. Technol. 8, 90–98. https://doi.org/10.25299/jgeet.2023.8.2.11651

Irwandi, Zulfakriza, Muzli, Hassan, H.M., Makoto Okubo, 2025. Seismic Hazard for Regional-Scale Sumatra Island Based on Realistic Physical Computation of Seismic Wave Propagation. J. Geosci. Eng. Environ. Technol. 10, 224–231. https://doi.org/10.25299/jgeet.2025.10.02.21751

Jones, E.S., Hayes, G.P., Bernardino, M., Dannemann, F.K.,

Furlong, K.P., Benz, H.M., Villaseñor, A., 2014. Seismicity of the Earth 1900-2012 Java and vicinity (No. 2010-1083- N), Open-File Report. U.S. Geological Survey. https://doi.org/10.3133/ofr20101083N

Karapetyan, J., Li, L., Zhou, J., Hovhannisyan, L., Wang, Y., Karapetyan, R., Gevorgyan, A., Harutyunyan, K., 2024. The Problems of Declustering in the Processing of Seismic Information in the Tauro Caucasus Region. Bull. Seismol. Soc. Am. 114, 2008–2027. https://doi.org/10.1785/0120230291

Khusnani, A., Anggraini, A., Jufriansah, A., Zulfakriza, Z., Pramudya, Y., Margiono, Wae, K.W., 2024. Relocation Study of Flores Sea Hypocenter (Mw = 7.3) Based on Single Station Estimation Using ObsPy. J. Geosci. Eng. Environ. Technol. 9, 113–120. https://doi.org/10.25299/jgeet.2024.9.2.14503

Kijko, A., 1988. Maximum likelihood estimation of Gutenberg-Richter b parameter for uncertain magnitude values. Pure Appl. Geophys. PAGEOPH 127, 573–579. https://doi.org/10.1007/BF00881745

Kijko, A., Sellevoll, M.A., 1990. Estimation of earthquake hazard parameters for incomplete and uncertain data files. Nat. Hazards 3, 1–13. https://doi.org/10.1007/BF00144970

Kim, K., Kaviari, F., Pant, P., Yamashita, E., 2022. An agent-based model of short-notice tsunami evacuation in Waikiki, Hawaii. Transp. Res. Part Transp. Environ. 105, 103239. https://doi.org/10.1016/j.trd.2022.103239

Laksono, F.A.T., Widagdo, A., Aditama, M.R., Fauzan, M.R., Kovács, J., 2022. Tsunami Hazard Zone and Multiple Scenarios of Tsunami Evacuation Route at Jetis Beach, Cilacap Regency, Indonesia. Sustainability 14, 2726. https://doi.org/10.3390/su14052726

Mayasari, Z.M., Afandi, N., 2021. OPTIMASI JALUR EVAKUASI BAGI PEJALAN KAKI MENGGUNAKAN ALGORITMA FUZZY DIJKSTRA DI KECAMATAN TELUK SEGARA, BENGKULU. BAREKENG J. Ilmu Mat. Dan Terap. 15, 581–590. https://doi.org/10.30598/barekengvol15iss3pp581-590

Newcomb, K.R., McCann, W.R., 1987. Seismic history and seismotectonics of the Sunda Arc. J. Geophys. Res. Solid Earth 92, 421–439. https://doi.org/10.1029/JB092iB01p00421

Péroche, M., Leone, F., Gutton, R., 2014. An accessibility graph-based model to optimize tsunami evacuation sites and routes in Martinique, France. Adv. Geosci. 38, 1–8. https://doi.org/10.5194/adgeo-38-1-2014

Priadi, R., Yunus, D., Yonanda, B., Margiono, R., 2020. Analysis of Tsunami Inundation due in Pangandaran Tsunami Earthquake in South Java Area Based on Finite Faults Solutions Model. J. Penelit. Fis. Dan Apl. JPFA 10, 114. https://doi.org/10.26740/jpfa.v10n2.p114-124

Pristiwantoro, R.N.Z., Fahrudin, Widiarso, D.A., Moechtar, R.A.T., Cita, A., 2025. Active Tectonics of the Garsela Fault Utilizing Morphotectonics and Seismicity in Garut Regency, Indonesia. J. Geosci. Eng. Environ. Technol. 10, 119–125. https://doi.org/10.25299/jgeet.2025.10.02.20209

Reasenberg, P., 1985. Second-order moment of central California seismicity, 1969–1982. J. Geophys. Res. Solid Earth 90, 5479–5495. https://doi.org/10.1029/JB090iB07p05479

Sihombing, S., Sudarmaji, Sunardi, B., Darmawan, H., 2024. Tsunami Modeling Using DEMNAS and DEM Data from UAV Surveys for Planning Evacuation Routes on Samas Coast, Bantul Regency. J. Geosci. Eng. Environ. Technol. 9, 152–157. https://doi.org/10.25299/jgeet.2024.9.2.14777

Sriyanto, S.P.D., Adriano, B., Fujii, Y., Koshimura, S., 2025. Estimation of high-resolution tsunami inundation depth using deep learning models: Case study of Pangandaran, Indonesia. Ocean Eng. 330, 121019. https://doi.org/10.1016/j.oceaneng.2025.121019

Suananda Y., I.B., Aufa, I., Harlianti, U., 2018. Identifying Intraplate Mechanism by B-Value Calculations in the South of Java Island. IOP Conf. Ser. Earth Environ. Sci. 132, 012032. https://doi.org/10.1088/1755-1315/132/1/012032

Suardi, I., Afnimar, Widiyantoro, S., Yagi, Y., 2014. Moment Tensor Analysis of the September 2, 2009 Tasikmalaya, West Java Earthquake Using the Waveform Inversion Method of Near Field Data. Int. J. Tomogr. Simulation™ 25, 63–74.

Sularno, Mulya, D.P., Astri, R., 2021. Tsunami evacuation Geographic Information System (GIS) education as disaster mitigation. IOP Conf. Ser. Earth Environ. Sci. 708, 012004. https://doi.org/10.1088/1755-1315/708/1/012004

Supendi, P., Widiyantoro, S., Rawlinson, N., Yatimantoro, T., Muhari, A., Hanifa, N.R., Gunawan, E., Shiddiqi, H.A., Imran, I., Anugrah, S.D., Daryono, D., Prayitno, B.S., Adi, S.P., Karnawati, D., Faizal, L., Damanik, R., 2023. On the potential for megathrust earthquakes and tsunamis off the southern coast of West Java and southeast Sumatra, Indonesia. Nat. Hazards 116, 1315–1328. https://doi.org/10.1007/s11069-022-05696-y

Tahri, A., Beroho, M., Tichli, S., El Talibi, H., El Moussaoui, S., Aboumaria, K., 2025. Combining GIS and machine learning for enhanced tsunami risk management: A review of current approaches and unexplored future potential. E3S Web Conf. 607, 04025. https://doi.org/10.1051/e3sconf/202560704025

Tri Laksono, F.A., Aditama, M.R., Setijadi, R., Ramadhan, G., 2020. Run-up Height and Flow Depth Simulation of the 2006 South Java Tsunami Using COMCOT on Widarapayung Beach. IOP Conf. Ser. Mater. Sci. Eng. 982, 012047. https://doi.org/10.1088/1757-899x/982/1/012047

Windupranata, W., Hanifa, N.R., Nusantara, C.A.D.S., Aristawati, G., Arifianto, M.R., 2020. Analysis of tsunami hazard in the Southern Coast of West Java Province - Indonesia. IOP Conf. Ser. Earth Environ. Sci. 618, 012026. https://doi.org/10.1088/1755-1315/618/1/012026

Zikky, Moh., 2016. Review of A* (A Star) Navigation Mesh Pathfinding as the Alternative of Artificial Intelligent for Ghosts Agent on the Pacman Game. Emit. Int. J. Eng. Technol. 4. https://doi.org/10.24003/emitter.v4i1.117